Article:
Li, Y, He, Y, Sun, Y et al. (2019) Solving the Vlasov–Maxwell equations using Hamiltonian splitting. Journal of Computational Physics, 396. pp. 381-399. ISSN: 0021-9991

https://doi.org/10.1016/j.jcp.2019.06.070

Solving the Vlasov–Maxwell equations using Hamiltonian splitting

Yingzhe Li[a,b], Yang He[c], Yajuan Sun[a,b,*], Jitse Niesen[d], Hong Qin[e,f], Jian Liu[e,g]

[a] *LSEC, ICMSEC, Academy of Mathematics and Systems Science, Chinese Academy of Sciences, Beijing 100190, CHINA*
[b] *School of Mathematical Sciences, University of Chinese Academy of Sciences, Beijing 100049, CHINA*
[c] *School of Mathematics and Physics, University of Science and Technology Beijing, Beijing 100083, CHINA*
[d] *Department of Applied Mathematics, University of Leeds, Leeds LS2 9JT, UK*
[e] *Department of Engineering and Applied Physics, University of Science and Technology of China, Hefei, Anhui 230026, CHINA*
[f] *Plasma Physics Laboratory, Princeton University, Princeton, NJ 08543, USA*
[g] *Key Laboratory of Geospace Environment, CAS, Hefei, Anhui 230026, People's Republic of China*

Abstract

In this paper, the numerical discretizations based on Hamiltonian splitting for solving the Vlasov–Maxwell system are constructed. We reformulate the Vlasov–Maxwell system in Morrison–Marsden–Weinstein Poisson bracket form. Then the Hamiltonian of this system is split into five parts, with which five corresponding Hamiltonian subsystems are obtained. The splitting method in time is derived by composing the solutions to these five subsystems. Combining the splitting method in time with the Fourier spectral method and finite volume method in space gives the full numerical discretizations which possess good conservation for the conserved quantities including energy, momentum, charge, etc. In numerical experiments, we simulate the Landau damping, Weibel instability and Bernstein wave to verify the numerical algorithms.

Keywords: Vlasov–Maxwell system, Poisson bracket, Hamiltonian splitting

*Corresponding author
Email address: sunyj@lsec.cc.ac.cn (Yajuan Sun)

method.

1. Introduction

In modern plasma physics and accelerator physics, the system of Vlasov–Maxwell (VM) equations is an important model to describe collisionless plasma. In most applications such as radio-frequency wave heating, current drive in tokamaks, etc., this system usually involves a wide range of space and time scales, which requires long-time numerical simulation. Classical algorithms, however, can not control the rapid accumulation of numerical errors which soon destroy the numerical simulation completely. Therefore, the challenging task for simulating the VM system is to construct efficient and accurate numerical methods with long-term stability.

To numerically solve the VM equations, Particle-in-Cell (PIC) method has been an important tool in the last half century [1, 2, 11]. The main idea of this method is to approximate the distribution function by a collection of finite-size "quasi-particles" with the weighted Klimontovich representation. The particles are advanced along the characteristics of the Vlasov equation, and the electromagnetic field is computed by using a mesh in the physical space. The advantage of PIC method is its low computational cost, thus it is suitable to solve high-dimensional problems. The PIC method has also been developed by combining with the geometric integrators, and applied to the VM system [14, 25, 32, 44, 38]. However, PIC method suffers from numerical noises which results in poor description for low-density regions. Moreover, the numerical noise decreases in $1/\sqrt{N}$, when the number of particles N is increased. Besides the PIC method, there are deterministic methods for solving the VM system, such as the semi-Lagrangian methods [10, 37], the finite volume methods [17], the spectral methods [26], the finite element methods [13, 23], etc. In some cases, for example, when particles in the tail of the distribution play an important role, or when the numerical noise becomes too evident, deterministic methods are much better than PIC methods. Recently, some energy conserving methods have been proposed for Vlasov system in [6, 7, 8].

Geometric numerical integrators [16, 20, 34] have been proposed with the purpose of preserving the intrinsic properties inherited by the given system. Via preserving the properties of system such as the Poisson structure of Hamiltonian system and the invariant volume form of source-free system,

geometric integration methods usually generate numerical results with superior long-term behavior compared to others. The VM system is known to be a non-canonical Hamiltonian system with Poisson bracket [29, 41, 27]. This implies that its solution flow is a Poisson map, and the system has Casimir functions and many conserved quantities. Thus, it is significant to construct numerical methods which can preserve the Poisson structure. In construction of Poisson-preserving numerical methods, splitting approach has been widely used. Splitting approach is a useful method in designing geometric numerical methods, e.g. symplectic methods, Poisson methods, volume-preserving methods, and first integral preserving methods [20, 33], etc. They have been developed for solving the charged particle system [21, 22], and the Schrödinger equation [3, 15]. Moreover, splitting methods are also applied to the VM system [9, 35]. However, it has been pointed out in [31] that the method in [9] is not a Poisson-preserving method as the bracket used is not Poisson [41].

In this paper, we construct the Poisson-preserving methods for the VM system by Hamiltonian splitting. Based on Hamiltonian formulation of VM system, the Hamiltonian of this system is split into five parts with which five Hamiltonian subsystems are obtained. The approximate solution of the VM equations finally can be constructed by composing the solutions of each subsystem. Moreover, the evolution of the distribution function can be written as a composition of several one-dimensional advections, which makes the method efficient and easy to implement. It is also proved that the semi-discretized approximate solutions computed by our method preserve the Poisson structure, and also satisfy the Gauss's laws.

The framework of this paper is organized as follows. In section 2, we introduce the Hamiltonian structure and conserved quantities of the Vlasov–Maxwell equations. In section 3, the Hamiltonian splitting method is proposed. In section 4, we obtain a full discretization for the reduced VM system by combining the spectral method and the finite volume method in space. Section 5 is concerned with numerical experiments exploring Landau damping, the Weibel instability and Bernstein wave, and section 6 contains the concluding remarks and future works.

2. The Vlasov–Maxwell equations

The Vlasov–Maxwell equations describe collisionless magnetized charged particles in an electromagnetic field which can be either self-consistent, i.e.,

generated by the particles themselves or externally applied. As the ions have much greater inertia than the electrons, in this paper the ions are treated as a uniform fixed background. Then, the evolution of a single species of non-relativistic electrons under the self-consistent electromagnetic field is described as

$$\begin{aligned} \frac{\partial f}{\partial t} + \mathbf{v} \cdot \frac{\partial f}{\partial \mathbf{x}} + \frac{e}{m} (\mathbf{E} + \mathbf{v} \times \mathbf{B}) \cdot \frac{\partial f}{\partial \mathbf{v}} = 0, \\ \nabla \times \mathbf{B} = \mu_0 \mathbf{J}(\mathbf{x}, t) + \varepsilon_0 \mu_0 \frac{\partial \mathbf{E}}{\partial t}, \\ \nabla \times \mathbf{E} = -\frac{\partial \mathbf{B}}{\partial t}, \\ \nabla \cdot \mathbf{E} = \frac{\rho(\mathbf{x}, t)}{\varepsilon_0} + \frac{\rho_i}{\varepsilon_0}, \\ \nabla \cdot \mathbf{B} = 0, \end{aligned} \tag{1}$$

where $\mathbf{J}(\mathbf{x}, t) = e \int_{\mathbb{R}^3} f(\mathbf{x}, \mathbf{v}, t) \mathbf{v} \, d\mathbf{v}$ and $\rho(\mathbf{x}, t) = e \int_{\mathbb{R}^3} f(\mathbf{x}, \mathbf{v}, t) \, d\mathbf{v}$. The above equations are defined on $\Omega = \Omega_{\mathbf{x}} \times \mathbb{R}^3$ with $\mathbf{x} \in \Omega_{\mathbf{x}} \subset \mathbb{R}^3$ the position in physical space, and $\mathbf{v} \in \mathbb{R}^3$ the velocity. Here m is the electron mass, e is the electron charge, μ_0 is the magnetic permeability, ε_0 is the vacuum permittivity, $f(\mathbf{x}, \mathbf{v}, t) \geq 0$ is the electron distribution function, $\rho(\mathbf{x}, t)$ is the charge density of electrons, ρ_i is a constant charge density of ions, $\mathbf{J}(\mathbf{x}, t)$ is the electric current, and $\mathbf{E}(\mathbf{x}, t)$ and $\mathbf{B}(\mathbf{x}, t)$ are the electric and magnetic fields respectively. By requiring $\iint_\Omega \rho(\mathbf{x}, t) + \rho_i \, d\mathbf{x} = 0$, the total charge neutrality of system (1) is ensured.

Let $\omega_\rho = (ne^2/m\varepsilon_0)^{1/2}$ be the electron plasma frequency with the total number of electrons $n = \iint_\Omega f(\mathbf{x}, \mathbf{v}, t) \, d\mathbf{x} \, d\mathbf{v}$. We consider the normalized VM system where $(t, \mathbf{x}, \mathbf{v}, f, \mathbf{E}, \mathbf{B})$ is normalized by $(\omega_\rho^{-1}, c\omega_\rho^{-1}, c, n/c^3, \omega_\rho cm/e, \omega_\rho m/e)$ with c the speed of light in vacuum [6]. This yields the dimensionless non-relativistic Vlasov–Maxwell system:

$$\frac{\partial f}{\partial t} + \mathbf{v} \cdot \frac{\partial f}{\partial \mathbf{x}} + (\mathbf{E} + \mathbf{v} \times \mathbf{B}) \cdot \frac{\partial f}{\partial \mathbf{v}} = 0, \tag{2}$$

$$\frac{\partial \mathbf{E}}{\partial t} = \nabla \times \mathbf{B} - \mathbf{J}, \tag{3}$$

$$\frac{\partial \mathbf{B}}{\partial t} = -\nabla \times \mathbf{E}, \tag{4}$$

$$\nabla \cdot \mathbf{E} = \rho - 1, \tag{5}$$

$$\nabla \cdot \mathbf{B} = 0, \tag{6}$$

where $\mathbf{J}(\mathbf{x},t)$ and $\rho(\mathbf{x},t)$ are normalized as $\mathbf{J}(\mathbf{x},t) = \int_{\mathbb{R}^3} f(\mathbf{x},\mathbf{v},t)\mathbf{v}d\mathbf{v}$ and $\rho(\mathbf{x},t) = \int_{\mathbb{R}^3} f(\mathbf{x},\mathbf{v},t)d\mathbf{v}$.

It is known that equations (2)–(6) are not independent, as equations of Gauss's laws (5)–(6) can be derived from (2)–(4). Indeed, taking the divergence of both sides of (4) we derive

$$\frac{\partial}{\partial t}\left(\nabla\cdot\mathbf{B}\right) = 0. \tag{7}$$

Similarly, taking the divergence of both sides of (3) gives

$$\frac{\partial}{\partial t}\nabla\cdot\mathbf{E} + \int_{\mathbb{R}^3}\mathbf{v}\cdot\frac{\partial f}{\partial \mathbf{x}}\,d\mathbf{v} = 0. \tag{8}$$

By using (2), from (8) we obtain

$$\frac{\partial}{\partial t}\nabla\cdot\mathbf{E} - \int_{\mathbb{R}^3}\frac{\partial f}{\partial t}\,d\mathbf{v} - \int_{\mathbb{R}^3}\left(\mathbf{E}+\mathbf{v}\times\mathbf{B}\right)\cdot\frac{\partial f}{\partial \mathbf{v}}\,d\mathbf{v} = 0. \tag{9}$$

If we assume $f(\mathbf{x},\mathbf{v},t)$ is compactly supported in the velocity direction, then the third term of (9) vanishes after integration by parts, which leads to

$$\frac{\partial}{\partial t}\left(\nabla\cdot\mathbf{E} - \int_{\mathbb{R}^3} f\,d\mathbf{v}\right) = 0. \tag{10}$$

If an appropriate initial condition is imposed, it is clear that Eqs. (5)–(6) can be derived directly from (7) and (10).

Denote by $\mathcal{M}$ the infinite-dimensional manifold $\{(f,\mathbf{E},\mathbf{B})|\,\nabla\cdot\mathbf{B}=0\}$. In this paper, we consider the Vlasov–Maxwell system expressed with the below Poisson bracket [27] for the purpose of applying the ideas of geometric numerical integration [20]. For two functionals $\mathcal{F}$ and $\mathcal{G}$ on $\mathcal{M}$, the bracket is defined [29, 27] as

$$\begin{aligned}\{\mathcal{F},\mathcal{G}\} = &\iint_\Omega f\left[\frac{\delta\mathcal{F}}{\delta f},\frac{\delta\mathcal{G}}{\delta f}\right]_{\mathbf{xv}} d\mathbf{x}\,d\mathbf{v} + \iint_\Omega\left(\frac{\delta\mathcal{F}}{\delta\mathbf{E}}\cdot\frac{\partial f}{\partial\mathbf{v}}\frac{\delta\mathcal{G}}{\delta f} - \frac{\delta\mathcal{G}}{\delta\mathbf{E}}\cdot\frac{\partial f}{\partial\mathbf{v}}\frac{\delta\mathcal{F}}{\delta f}\right)d\mathbf{x}\,d\mathbf{v}\\ &+\int_{\Omega_{\mathbf{x}}}\left(\frac{\delta\mathcal{F}}{\delta\mathbf{E}}\cdot\left(\nabla\times\frac{\delta\mathcal{G}}{\delta\mathbf{B}}\right) - \frac{\delta\mathcal{G}}{\delta\mathbf{E}}\cdot\left(\nabla\times\frac{\delta\mathcal{F}}{\delta\mathbf{B}}\right)\right)d\mathbf{x}\\ &+\iint_\Omega f\mathbf{B}\cdot\left(\frac{\partial}{\partial\mathbf{v}}\frac{\delta\mathcal{F}}{\delta f}\times\frac{\partial}{\partial\mathbf{v}}\frac{\delta\mathcal{G}}{\delta f}\right)d\mathbf{x}\,d\mathbf{v},\end{aligned} \tag{11}$$

where $[\cdot,\cdot]_{\mathbf{xv}}$ denotes the canonical Lie bracket of two functions of $(\mathbf{x},\mathbf{v})$, i.e., $[h,g]_{\mathbf{xv}} = \sum_{i=1}^{3}\big(\frac{\partial h}{\partial x_i}\frac{\partial g}{\partial v_i} - \frac{\partial h}{\partial v_i}\frac{\partial g}{\partial x_i}\big)$. It has been proved in [27, 30] that the bracket (11) is Poisson. With the defined Poisson bracket, the Vlasov–Maxwell system of equations (2)–(4) is equivalent to

$$\frac{\partial \mathcal{Z}}{\partial t} = \{\mathcal{Z},\mathcal{H}\}, \tag{12}$$

with $\mathcal{Z} = (f,\mathbf{E},\mathbf{B}) \in \mathcal{M}$, where the Hamiltonian functional is defined by

$$\mathcal{H}(f,\mathbf{E},\mathbf{B}) = \frac{1}{2}\int_{\Omega}\mathbf{v}^2 f d\mathbf{x}d\mathbf{v} + \frac{1}{2}\int_{\Omega_{\mathbf{x}}}\left(|\mathbf{E}|^2+|\mathbf{B}|^2\right)d\mathbf{x}. \tag{13}$$

Note that Eq. (2) can also be written in conservative form

$$\frac{\partial f}{\partial t} + \nabla_{\mathbf{xv}}\cdot(\boldsymbol{\kappa} f) = 0, \tag{14}$$

where the phase space velocity vector is $\boldsymbol{\kappa} = (\mathbf{v}, \mathbf{E}+\mathbf{v}\times\mathbf{B})$, and $\nabla_{\mathbf{xv}} = (\nabla_{\mathbf{x}},\nabla_{\mathbf{v}})$ denotes the gradient operator in phase space. There are numerical methods derived from this conservative formulation [18, 10].

With appropriate initial conditions $(f_0(\mathbf{x},\mathbf{v}),\mathbf{E}_0(\mathbf{x}),\ \mathbf{B}_0(\mathbf{x})) \in \mathcal{M}$, the existence and uniqueness of a local solution for the VM equations have been proved in [42], and the global existence without uniqueness of the weak solution has been proved in [12]. As a system from plasma physics, the VM system is known to have a number of conservative quantities among which the several important ones are reviewed as follows.

Proposition 2.1. *Consider the Vlasov–Maxwell system (2)–(6). If $f(\mathbf{x},\mathbf{v},t)$, $\mathbf{E}(\mathbf{x},t)$, and $\mathbf{B}(\mathbf{x},t)$ are periodic in $\mathbf{x}$, and f is compactly supported in $\mathbf{v}$, then the following quantities are conserved:*

(i). The energy $\mathcal{E} = \frac{1}{2}\iint_{\Omega} f|\mathbf{v}|^2\,d\mathbf{v}\,d\mathbf{x} + \frac{1}{2}\int_{\Omega_{\mathbf{x}}}\left(|\mathbf{E}|^2+|\mathbf{B}|^2\right)d\mathbf{x}$;

(ii). The charge $\mathcal{Q} = \iint_{\Omega} f(\mathbf{x},\mathbf{v},t)\,d\mathbf{v}\,d\mathbf{x}$;

(iii). The L^p–norm of the distribution function, $\left(\iint_{\Omega}|f|^p\,d\mathbf{v}\,d\mathbf{x}\right)^{1/p}$, *for* $1 \le p \le +\infty$;

(iv). The entropy $\mathcal{S} = -\iint_{\Omega} f\ln f\,d\mathbf{v}\,d\mathbf{x}$.

PROOF. *(i). The energy conservation is obvious because the energy $\mathcal{E}$ is actually the Hamiltonian (13) of the VM system.*

(ii). Integrating (2) over $\mathbf{x}$ *and* $\mathbf{v}$ *yields*

$$\iint_\Omega \frac{\partial f}{\partial t}\, d\mathbf{x}\, d\mathbf{v} = -\int_{\mathbb{R}^3} \mathbf{v}\cdot\left(\int_{\Omega_\mathbf{x}} \frac{\partial f}{\partial \mathbf{x}} d\mathbf{x}\right) d\mathbf{v} - \iint_\Omega (\mathbf{E}+\mathbf{v}\times\mathbf{B})\cdot\frac{\partial f}{\partial \mathbf{v}}\, d\mathbf{x}\, d\mathbf{v}. \tag{15}$$

Because f is periodic in $\mathbf{x}$, the first term on the right-hand side is zero. The assumption of f having compact support in the velocity directions implies that the second term on the right-hand side of (15) also vanishes. This leads to

$$\frac{d\mathcal{Q}}{dt} = \frac{d}{dt}\iint_\Omega f(\mathbf{x},\mathbf{v},t)\, d\mathbf{v}\, d\mathbf{x} = 0,$$

which implies the conservation of charge.

(iii). We multiply (2) by pf^{p-1} and integrate over Ω to obtain

$$\frac{d}{dt}\iint_\Omega f^p\, d\mathbf{x}\, d\mathbf{v} = -\int_{\mathbb{R}^3} \mathbf{v}\cdot\left(\int_{\Omega_\mathbf{x}} \frac{\partial f^p}{\partial \mathbf{x}} d\mathbf{x}\right) d\mathbf{v} - \iint_\Omega (\mathbf{E}+\mathbf{v}\times\mathbf{B})\cdot\frac{\partial f^p}{\partial \mathbf{v}}\, d\mathbf{x}\, d\mathbf{v}. \tag{16}$$

Similarly as in (ii), the right-hand side of (16) vanishes.

(iv.) As in the proof of (iii), multiplying (2) by $\ln f + 1$ and integrating over Ω gives the desired conservation law.

□

In this paper, as we take ions as the uniform fixed background, the classical momentum

$$\mathbf{M} = \iint_\Omega \mathbf{v} f\, d\mathbf{v}\, d\mathbf{x} + \int_{\Omega_x} \mathbf{E}\times\mathbf{B}\, d\mathbf{x} \tag{17}$$

can not be conserved [8]. For two species (electrons and ions) Vlasov–Maxwell system, the following momentum with incorporating the motion of ions

$$\mathcal{P} = \iint_\Omega \mathbf{v}\left(f + \frac{m_i}{m} f_i\right) d\mathbf{v}\, d\mathbf{x} + \int_{\Omega_x} \mathbf{E}\times\mathbf{B}\, d\mathbf{x},$$

where f_i is the distribution function of ions and m_i is their mass, is conserved.

Proposition 2.2. *Define*

$$\mathcal{C}_{\mathbf{x}_0}(f,\mathbf{E},\mathbf{B}) = \int_{\Omega_x} \nabla\cdot\mathbf{E}(\mathbf{x})\delta(\mathbf{x}-\mathbf{x}_0)\,d\mathbf{x} - \iint_{\Omega} f(\mathbf{x},\mathbf{v},t)\delta(\mathbf{x}-\mathbf{x}_0)\,d\mathbf{x}\,d\mathbf{v}, \tag{18}$$

where $\mathbf{x}_0 \in \Omega_x$ and δ represents the delta function. Then, (18) is a Casimir function[1] *with respect to the Poisson bracket defined in (11).*

Proof. For the Poisson bracket defined in (11), we have

$$\begin{aligned}
&\{\mathcal{C}_{\mathbf{x}_0}(\mathcal{Z}),\mathcal{G}(\mathcal{Z})\}\\
&= \iint_{\Omega} f\left[-\delta(\mathbf{x}-\mathbf{x}_0),\frac{\delta\mathcal{G}}{\delta f}\right]_{\mathbf{xv}} d\mathbf{x}d\mathbf{v} + \iint_{\Omega}\left(-\nabla_{\mathbf{x}}\delta(\mathbf{x}-\mathbf{x}_0)\cdot\frac{\partial f}{\partial\mathbf{v}}\frac{\delta\mathcal{G}}{\delta f}\right)d\mathbf{x}d\mathbf{v}\\
&+ \iint_{\Omega}\left(\frac{\delta\mathcal{G}}{\delta\mathbf{E}}\cdot\frac{\partial f}{\partial\mathbf{v}}\delta(\mathbf{x}-\mathbf{x}_0)\right)d\mathbf{x}d\mathbf{v} + \int_{\Omega_x} -\nabla_{\mathbf{x}}\delta(\mathbf{x}-\mathbf{x}_0)\cdot\left(\nabla\times\frac{\delta\mathcal{G}}{\delta\mathbf{B}}\right)d\mathbf{x}.
\end{aligned} \tag{19}$$

In the above equality, we have used the following variational derivatives of $\mathcal{C}_{x_0}$,

$$\frac{\delta\mathcal{C}_{\mathbf{x}_0}}{\delta f} = -\delta(\mathbf{x}-\mathbf{x}_0), \quad \frac{\delta\mathcal{C}_{\mathbf{x}_0}}{\delta\mathbf{E}} = -\nabla_{\mathbf{x}}\delta(\mathbf{x}-\mathbf{x}_0), \quad \frac{\delta\mathcal{C}_{\mathbf{x}_0}}{\delta\mathbf{B}} = \mathbf{0}.$$

In (19), with the integration by parts the sum of the first and second terms is zero, and the integrand of the fourth term vanishes. Since f is compact supported in velocity direction, the third term is also zero. Then the proof is finished. □

Due to the conservation properties inherited by the VM system, it is important to construct the numerical discretizations which can preserve these conserved quantities (at least up to some tolerance; ideally up to machine precision) in long-time numerical simulations. In the subsequent sections, we present the numerical discretizations which preserve the Poisson bracket of the VM system, and the corresponding numerical simulations.

[1]For the given Poisson bracket $\{\ ,\ \}$, function $\mathcal{C}$ is a Casimir function if it Poisson commutes with any smooth function $\mathcal{G}$, i.e., $\{\mathcal{C},\mathcal{G}\}=0$.

3. Hamiltonian splitting methods for the VM equations

In this section, we introduce a Hamiltonian splitting method for the VM system based on its formulation written in (12). Observing the Hamiltonian (13) of the VM equations, we find that we can split the Hamiltonian $\mathcal{H}$ as

$$\begin{aligned}\mathcal{H} &= \frac{1}{2}\int |\mathbf{E}|^2 d\mathbf{x} + \frac{1}{2}\int |\mathbf{B}|^2 d\mathbf{x} + \frac{1}{2}\sum_{i=1}^{3}\int v_i^2 f d\mathbf{x} d\mathbf{v} \\ &=: \mathcal{H}_E + \mathcal{H}_B + \sum_{i=1}^{3}\mathcal{H}_{if}.\end{aligned} \tag{20}$$

Substituting (20) into (12) gives five subsystems of the Vlasov–Maxwell system (12) defined on $\mathcal{M}$:

$$\dot{\mathcal{Z}} = \{\mathcal{Z}, \mathcal{H}_E\}, \quad \dot{\mathcal{Z}} = \{\mathcal{Z}, \mathcal{H}_B\}, \quad \dot{\mathcal{Z}} = \{\mathcal{Z}, \mathcal{H}_{if}\} \text{ for } i = 1, 2, 3.$$

This Hamiltonian splitting enjoys the following properties: (i) it is Hamiltonian, i.e., each subsystem preserves the same Hamiltonian structure as the VM system; (ii) it is a conservative splitting, i.e., each subsystem can be written in conservative form like Eq. (14); (iii) the solution to each subsystem can be written explicitly; (iv) the distribution function $f(\mathbf{x}, \mathbf{v}, t)$ evolves by several one-dimensional translations.

We start with the first subsystem $\dot{\mathcal{Z}} = \{\mathcal{Z}, \mathcal{H}_E\}$, which is equivalent to

$$\begin{aligned}\frac{\partial f}{\partial t} + \mathbf{E}(\mathbf{x}, t) \cdot \frac{\partial f}{\partial \mathbf{v}} &= 0, \\ \frac{\partial \mathbf{E}}{\partial t} &= 0, \\ \frac{\partial \mathbf{B}}{\partial t} &= -\nabla \times \mathbf{E}.\end{aligned} \tag{21}$$

For given initial values $(f_0, \mathbf{E}_0, \mathbf{B}_0) \in \mathcal{M}$ at time $t = 0$, the solution to subsystem (21) at time t can be written explicitly as

$$\begin{aligned}f(\mathbf{x}, \mathbf{v}, t) &= f_0\left(\mathbf{x}, \mathbf{v} - t\mathbf{E}_0(\mathbf{x})\right), \\ \mathbf{E}(\mathbf{x}, t) &= \mathbf{E}_0(\mathbf{x}), \\ \mathbf{B}(\mathbf{x}, t) &= \mathbf{B}_0(\mathbf{x}) - t\nabla \times \mathbf{E}_0(\mathbf{x}).\end{aligned} \tag{22}$$

In fact, the evolution equation for f can be further split into three parts:

$$\frac{\partial f}{\partial t} + E_1 \frac{\partial f}{\partial v_1} = 0, \quad \frac{\partial f}{\partial t} + E_2 \frac{\partial f}{\partial v_2} = 0, \quad \frac{\partial f}{\partial t} + E_3 \frac{\partial f}{\partial v_3} = 0, \tag{23}$$

where $\mathbf{E}(\mathbf{x}, t) = [E_1, E_2, E_3]$. It is easy to verify that the Lie composition of the three solutions of (23) leads to the solution f in (22), i.e.,

$$f(\mathbf{x}, \mathbf{v}, t) = \mathcal{S}^E_{v_3}(t)\mathcal{S}^E_{v_2}(t)\mathcal{S}^E_{v_1}(t) f_0(\mathbf{x}, \mathbf{v}), \tag{24}$$

where the translation operator $\mathcal{S}^E_{v_i}(t), i = 1, 2, 3$ is defined as $\mathcal{S}^E_{v_i}(t)h(\mathbf{x}, \mathbf{v}) = h(\mathbf{x}, \mathbf{v} - tE_i\mathbf{e}_i)$ with $\mathbf{e}_i$ the unit vector in the i-th Cartesian direction.

The second subsystem, which corresponds to $\dot{\mathcal{Z}} = \{\mathcal{Z}, \mathcal{H}_B\}$, is given by

$$\begin{aligned} \frac{\partial f}{\partial t} &= 0, \\ \frac{\partial \mathbf{E}}{\partial t} &= \nabla \times \mathbf{B}, \\ \frac{\partial \mathbf{B}}{\partial t} &= 0. \end{aligned} \tag{25}$$

With the initial condition $(f_0, \mathbf{E}_0, \mathbf{B}_0) \in \mathcal{M}$, the solution to the subsystem (25) can be written explicitly as

$$\begin{aligned} f(\mathbf{x}, \mathbf{v}, t) &= f_0(\mathbf{x}, \mathbf{v}), \\ \mathbf{E}(\mathbf{x}, t) &= \mathbf{E}_0(\mathbf{x}) + t\nabla \times \mathbf{B}_0(\mathbf{x}), \\ \mathbf{B}(\mathbf{x}, t) &= \mathbf{B}_0(\mathbf{x}). \end{aligned} \tag{26}$$

The subsystem corresponding to $\mathcal{H}_{if}$ is

$$\begin{aligned} &\frac{\partial f}{\partial t} + v_i \frac{\partial f}{\partial x_i} + \sum_{j=1}^{3} \hat{B}_{ji} v_i \frac{\partial f}{\partial v_j} = 0, \\ &\frac{\partial E_i}{\partial t} = -\int v_i f \, d\mathbf{v} \quad \text{and} \quad \frac{\partial E_j}{\partial t} = 0 \quad \text{for} \quad j \neq i, \\ &\frac{\partial \mathbf{B}}{\partial t} = 0. \end{aligned} \tag{27}$$

Here, $\hat{\mathbf{B}} = \begin{bmatrix} 0 & B_3 & -B_2 \\ -B_3 & 0 & B_1 \\ B_2 & -B_1 & 0 \end{bmatrix}$ is a skew-symmetric matrix determined by $\mathbf{B}(\mathbf{x}, t) = [B_1, B_2, B_3]^\top$. From the third equation of (27), we know that $\mathbf{B}(\mathbf{x}, t)$ does

not depend on time. Thus, the characteristic equation of the first equation of (27) is

$$\begin{aligned} &\dot{x}_i = v_i, \qquad \dot{v}_i = 0, \\ &\dot{x}_j = 0, \qquad \dot{v}_j = \hat{B}_{ji}(\mathbf{x}, 0) v_i \quad \text{for} \quad j \neq i. \end{aligned}$$

The solution to these equations is

$$\begin{aligned} &x_i(t) = x_i(0) + t v_i(0), \qquad v_i(t) = v_i(0), \\ &x_j(t) = x_j(0), \qquad v_j(t) = v_j(0) + \int_{x_i(0)}^{x_i(t)} \hat{B}_{ji}(\mathbf{x}, 0)\, dx_i \quad \text{for} \quad j \neq i. \end{aligned} \tag{28}$$

With the initial condition $(f_0, \mathbf{E}_0, \mathbf{B}_0) \in \mathcal{M}$, this leads to the following exact solution to the subsystem $\mathcal{H}_{if}$:

$$\begin{aligned} f(\mathbf{x}, \mathbf{v}, t) = f_0 \left(\mathbf{x} - t v_i \mathbf{e}_i, \mathbf{v} - \sum_{l=1}^{3} \mathbf{e}_l F_l^{(i)} \right) \quad \text{with} \quad F_l^{(i)} = \int_{x_i - t v_i}^{x_i} \hat{B}_{li}(\mathbf{x}, 0)\, dx_i, \\ E_i(\mathbf{x}, t) = E_i(\mathbf{x}, 0) - \int_0^t \int v_i f(\mathbf{x}, \mathbf{v}, \tau)\, d\mathbf{v}\, d\tau, \\ \mathbf{B}(\mathbf{x}, t) = \mathbf{B}_0(\mathbf{x}), \qquad E_j(\mathbf{x}, t) = E_{0j}(\mathbf{x}) \quad \text{for} \quad j \neq i. \end{aligned}$$

Similarly as in the first subsystem, the distribution function $f(\mathbf{x}, \mathbf{v}, t)$ which solves (27) can also be expressed as three one-dimensional advections. Firstly, we translate f_0 in two velocity directions v_j and v_k, $j, k \neq i$, and obtain $f_0 \left(\mathbf{x}, \mathbf{v} - \sum_{l=1}^{3} \mathbf{e}_l \hat{F}_l^{(i)} \right)$, then we translate $-t v_i$ in the x_i-direction to get $f(\mathbf{x}, \mathbf{v}, t)$, i.e.,

$$f(\mathbf{x}, \mathbf{v}, t) = \mathcal{S}_{x_i}^{if}(t) \mathcal{S}_{v_j}^{if}(t) \mathcal{S}_{v_k}^{if}(t) f_0(\mathbf{x}, \mathbf{v}), \quad j, k \neq i, \tag{29}$$

where $\mathcal{S}_{x_i}^{if}(t) h(\mathbf{x}, \mathbf{v}) = h(\mathbf{x} - t v_i \mathbf{e}_i, \mathbf{v})$, and $\mathcal{S}_{v_j}^{if}(t) h(\mathbf{x}, \mathbf{v}) = h(\mathbf{x}, \mathbf{v} - \hat{F}_j^{(i)} \mathbf{e}_j)$ with $\hat{F}_j^{(i)} = \int_{x_i}^{x_i + t v_i} \hat{B}_{li}(\mathbf{x}, 0)\, dx_i$.

Combining the solutions of the above subsystems by various kinds of composition methods [20, 45, 40, 28] gives schemes of high order, e.g., the first-order Lie splitting method, the second-order Strang splitting method and so on.

Theorem 3.1. *Assume that the VM system is periodic in* $\mathbf{x}$*,* $f(\mathbf{x},\mathbf{v},t)$ *is compactly supported in* $\mathbf{v}$*, and the Gauss's Law is satisfied by initial conditions, then the solution given by Hamiltonian splitting method (semi-discretization in time) satisfies the Gauss's law.*

PROOF. *For the semi-discretization, it is sufficient to check whether Gauss's law holds for the solution of each subsystem. From the solution of each subsystem, it is obvious that* $\nabla\cdot\mathbf{B}=0$ *is satisfied by the solution of semi-discretization. As for* $\nabla\cdot\mathbf{E}=\iint_\Omega f\,d\mathbf{x}\,d\mathbf{v}-1$*, we first consider subsystem* $\mathcal{H}_E$ *(21). From (22) we know*

$$\int_{\mathbb{R}^3} f(\mathbf{x},\mathbf{v},t)\,d\mathbf{v}=\int_{\mathbb{R}^3} f_0\left(\mathbf{x},\mathbf{v}-t\mathbf{E}_0\left(\mathbf{x}\right)\right)d\mathbf{v}=\int_{\mathbb{R}^3} f_0(\mathbf{x},\mathbf{v})\,d\mathbf{v}\quad \textit{for all } x.$$

As $\mathbf{E}(\mathbf{x},t)$ *does not change along time, and* $\nabla\cdot\mathbf{E}_0(\mathbf{x})=\int_{\mathbb{R}^3} f_0(\mathbf{x},\mathbf{v})\,d\mathbf{v}-1$*, we derive*

$$\nabla\cdot\mathbf{E}(\mathbf{x},t)=\nabla\cdot\mathbf{E}_0(\mathbf{x})=\int_{\mathbb{R}^3} f(\mathbf{x},\mathbf{v},t)\,d\mathbf{v}-1.$$

For subsystem $\mathcal{H}_B$ *(25), taking the divergence of* $\mathbf{E}(\mathbf{x},t)$ *in (26) directly gives*

$$\nabla\cdot\mathbf{E}(\mathbf{x},t)=\nabla\cdot\mathbf{E}_0(\mathbf{x})+t\nabla\cdot\nabla\times\mathbf{B}_0(\mathbf{x})=\nabla\cdot\mathbf{E}_0(\mathbf{x}).$$

Notice that $f(\mathbf{x},\mathbf{v},t)$ *does not change along time, it is clear from the above equality that Gauss's law is satisfied by the solution of* $\mathcal{H}_B$*. Finally, we consider the* $\mathcal{H}_{if}$ *subsystem (27). Taking the derivative of the second equation in (27) with respect to* t*, gives*

$$\nabla\cdot\frac{\partial\mathbf{E}}{\partial t}=-\int_{\mathbb{R}^3}\sum_{i=1}^{3} v_i\frac{\partial f}{\partial x_i}\,d\mathbf{v}.$$

Substituting the first equation of (27) into the above equation gives

$$\frac{\partial}{\partial t}\nabla\cdot\mathbf{E}=\int_{\mathbb{R}^3}\left(\frac{\partial f}{\partial t}+\sum_{j=1}^{3}\hat{B}_{ji}v_i\frac{\partial f}{\partial v_j}\right)d\mathbf{v}.$$

As the distribution function $f(\mathbf{x},\mathbf{v},t)$ *is compactly supported, the second integral on right side of the above equality* $\int_{\mathbb{R}^3}\sum_j \hat{B}_{ji}v_i\frac{\partial f}{\partial v_j}\,d\mathbf{v}$ *vanishes, and then Gauss' law is satisfied by the solution of* $\mathcal{H}_{if}$*. Thus we have finished our proof.* □

4. Phase space discretizations

In this section, we study the phase space discretizations for the so-called $1+\frac{1}{2}$ dimensional VM equations [9] defined on $[0, L]\times\mathbb{R}^2$. In this formulation, the independent variables are x_1, v_1 and v_2, and the fields E_3, B_1 and B_2 are set to be zero:

$$\frac{\partial f}{\partial t} + v_1\frac{\partial f}{\partial x_1} + (E_1 + v_2 B_3)\frac{\partial f}{\partial v_1} + (E_2 - v_1 B_3)\frac{\partial f}{\partial v_2} = 0, \tag{30}$$

$$\frac{\partial E_1}{\partial t} = -\int_{\mathbb{R}^2} v_1 f \, dv_1 \, dv_2, \tag{31}$$

$$\frac{\partial E_2}{\partial t} = -\frac{\partial B_3}{\partial x_1} - \int_{\mathbb{R}^2} v_2 f \, dv_1 \, dv_2, \tag{32}$$

$$\frac{\partial B_3}{\partial t} = -\frac{\partial E_2}{\partial x_1}. \tag{33}$$

We consider the case that the system is periodic in the x_1-direction. The computation domain is taken as $\Omega = \Omega_x \times \Omega_v := [0, L] \times [-V_{1,L}, V_{1,R}] \times [-V_{2,L}, V_{2,R}]$ with $V_{1,L}, V_{1,R}, V_{2,L}$ and $V_{2,R}$ large enough such that f is sufficiently small near $\Omega_x \times \partial\Omega_v$. We use a uniform mesh defined as follows:

$$x_{1,j} = (j-1)\Delta x \quad \text{with} \quad \Delta x = L/M \quad \text{for} \quad j = 1, \ldots, M;$$

$$v_{i,\ell_i+\frac{1}{2}} = -V_{i,L} + \ell_i \Delta v_i \text{ with } \Delta v_i = \frac{V_{i,R} + V_{i,L}}{N_i} \text{ for } \ell_i = 0, \ldots, N_i,\ i = 1, 2.$$

Firstly, we discretize the electromagnetic fields (E_1, E_2, B_3) for which the grid number M is usually even. We use the notation $E_{1,j}(t)$ to denote the approximation of $E_1(x_1, t)$ at $(x_{1,j}, t)$. As E_1 is periodic in the x_1-direction, we use the spectral Fourier expansion to approximate E_1 which is expressed as

$$E_{1,j}(t) = \sum_{k=-M/2+1}^{M/2} \hat{E}_{1,k}(t) e^{2\pi i j k/M} \quad \text{for} \quad j = 1, \ldots, M. \tag{34}$$

We discretize E_2 and B_3 in the same way.

To discretize the distribution function f, we use a spectral representation in the x_1-direction and a finite volume discretization in the velocity directions. We discretize the distribution function f on Ω_v by taking the averages of f over the rectangular cells $V_{\ell_1,\ell_2} := [v_{\ell_1-\frac{1}{2}}, v_{\ell_1+\frac{1}{2}}] \times [v_{\ell_2-\frac{1}{2}}, v_{\ell_2+\frac{1}{2}}]$ as our discrete

variables at velocity direction

$$f_{\ell_1,\ell_2}(x_1,t)=\frac{1}{\Delta v_1\Delta v_2}\iint_{V_{\ell_1,\ell_2}} f(x_1,v_1,v_2,t)\,dv_2\,dv_1 \text{ for } \ell_i=1,\ldots,N_i,\ i=1,2.$$

Similar to (34), we have

$$f_{j,\ell_1,\ell_2}(t)=\sum_{k=-M/2+1}^{M/2}\hat{f}_{k,\ell_1,\ell_2}e^{2\pi \mathrm{i} jk/M}\quad \text{for}\quad j=1,\ldots,M.$$

In order to evaluate the value of f off-grid in the v_1 (or v_2) direction, here we reconstruct a continuous function from the discrete value f_{j,ℓ_1,ℓ_2} by using the Parabolic Spline Method (PSM) introduced in [46]. It is proved in [46, 10] that the method has good accuracy, high efficiency and mass conservation property. It is also proved that the reconstruction by PSM is equivalent to apply the cubic spline interpolation to the primitive function with cumulative averages. From the analysis in previous section, we know that the implementation of splitting method only needs 1D translations. This implies that we only need the one-dimensional PSM in the purpose of approximating distribution function f by a continuous function.

Let $[a,b]$ be an interval, and assume that it is divided into N equal parts with $v_i=a+ih$ for $i=0,1,\cdots,N$, where $\Delta v=(b-a)/N$. As follows, we introduce the PSM by approximating the function f from the integral averages of f on each cell $[v_i,v_{i+1}]$, $f_i:=\int_{v_i}^{v_{i+1}} f(v)dv/\Delta v, i=0,\cdots,N-1$. For the given f_i, the PSM gives a piecewise quadratic polynomial $F(v)$ which is continuously differentiable on $[a,b]$,

$$F(v)=p_i\left(\frac{v-v_i}{\Delta v}\right)\text{ for } v\in[v_i,v_{i+1}],\quad i=0,\cdots,N-1,$$

where $p_i(v)=\alpha_i v^2+\beta_i v+\gamma_i$ with α_i, β_i and γ_i the coefficients. The $3N$ coefficients of function $F(v)$ are derived by requiring the following conditions,

$$\int_{[v_i,v_{i+1}]}F(v)dv/\Delta v=\int_0^1 p_i(v)dv=f_i,\quad i=0,\cdots,N-1, \tag{35}$$

$$p_i(1)=p_{i+1}(0),\quad p_{N-1}(1)=p_0(0),\quad i=0,\cdots,N-2, \tag{36}$$

$$p_i'(1)=p_{i+1}'(0),\quad p_{N-1}'(1)=p_0'(0),\quad i=0,\cdots,N-2, \tag{37}$$

where conditions (36) and (37) imply that $F(v)$ and $F'(v)$ are continuous at $v_i, i = 0, \cdots, N-1$. Instead of directly solving the above $3N$ equations, the coefficients of $F(v)$ can be determined by solving two N dimensional linear systems. The first equation satisfied by γ_i is written in matrix form

$$A\gamma = \mathbf{f}$$

with

$$A = \begin{pmatrix} 4 & 1 & 0 & \cdots & 0 & 1 \\ 1 & 4 & 1 & 0 & \cdots & 0 \\ 0 & 1 & 4 & 1 & \ddots & \vdots \\ \vdots & \ddots & \ddots & \ddots & \ddots & 0 \\ 0 & \cdots & 0 & 1 & 4 & 1 \\ 1 & 0 & \cdots & 0 & 1 & 4 \end{pmatrix}, \ \gamma = \begin{pmatrix} \gamma_0 \\ \vdots \\ \gamma_{N-1} \end{pmatrix} \text{ and } \mathbf{f} = 3 \begin{pmatrix} f_{N_1} + f_0 \\ \vdots \\ f_k + f_{k+1} \\ \vdots \\ f_{N-2} + f_{N-1} \end{pmatrix}.$$

The second equation for β_i is

$$B\beta = \mathbf{g},$$

$$B = \begin{pmatrix} 2 & 1 & 0 & \cdots & 0 & 0 \\ 0 & 2 & 1 & 0 & \cdots & 0 \\ 0 & 0 & 2 & 1 & \ddots & \vdots \\ \vdots & \ddots & \ddots & \ddots & \ddots & 0 \\ 0 & \cdots & 0 & 0 & 2 & 1 \\ 1 & 0 & \cdots & 0 & 0 & 2 \end{pmatrix}, \ \beta = \begin{pmatrix} \beta_0 \\ \vdots \\ \beta_{N-1} \end{pmatrix}, \mathbf{g} = 6 \begin{pmatrix} f_0 - \gamma_0 \\ \vdots \\ f_k - \gamma_k \\ \vdots \\ f_{N-1} - \gamma_{N-1} \end{pmatrix}. \tag{38}$$

The coefficients α_i can be derived by $\alpha_i = \frac{\beta_{i+1} - \beta_i}{2}$ for $i = 0, \cdots, N-2$, and $\alpha_{N-1} = \frac{\beta_1 - \beta_{N-1}}{2}$. By using the fast solver in [36], the above two linear systems $A\gamma = \mathbf{f}$ and $B\beta = \mathbf{g}$ can be solved with the cost of $\mathcal{O}(N)$. Note that we here use PSM with periodic boundary condition, PSM with natural boundary condition can also be used, and there is also fast solver [36, 46].

Remark 1. *As noticed above, the Hamiltonian splitting is also a conservative splitting, which means that if we want to construct the charge-preserving methods, we can use the conservative methods presented in [18, 10] to solve each subsystem.*

Using the Hamiltonian splitting method introduced in Section 3 and phase space discretization in Section 4, we now present the discrete solution to the corresponding subsystems $\mathcal{H}_E$ and $\mathcal{H}_{1f}$ of the reduced VM system (30)–(33). As the computation of $\mathcal{H}_{2f}$ is similar to $\mathcal{H}_E$, we omit it here.

Algorithm 1 Procedure for computing $f(\mathbf{x}, \mathbf{v}, t)$ in subsystem $\mathcal{H}_E$

Input: $f_{j,\ell_1,\ell_2}(0), \hat{E}_1(0), \hat{E}_2(0)$

1: **for** $j = 1$ to M **do**
2: **for** $\ell_1 = 1$ to N_1 **do**
3: obtain $f_{j,\ell_2}(v_2)$ by using PSM with $[f_{j,\ell_1,1}(0), \ldots, f_{j,\ell_1,N_2}(0)]$
4: compute $E_2(x_j)$ by using inverse FFT on $\hat{E}_2(0)$
5: obtain $f_{j,\ell_1}(v_2 - tE_2(x_j))$ by translating $f_{j,\ell_1}(v_2)$
6: compute the average of $f_{j,\ell_1}(v_2 - tE_2(x_j))$ along v_2 to obtain f^1_{j,ℓ_1,ℓ_2}
7: **end for**
8: **end for**
9: repeat the above procedure on f^1_{j,ℓ_1,ℓ_2} in the v_1-direction for $j = 1, \ldots, M$ and $l_2 = 1, \ldots, N_2$ to obtain $f_{j,\ell_1,\ell_2}(t)$

Output: $f_{j,\ell_1,\ell_2}(t)$

Subsystem of $\mathcal{H}_E$. In $1 + \frac{1}{2}$ dimensions, the subsystem corresponding to $\mathcal{H}_E$ turns into

$$\frac{\partial f}{\partial t} + E_1 \frac{\partial f}{\partial v_1} + E_2 \frac{\partial f}{\partial v_2} = 0, \qquad \frac{\partial E_1}{\partial t} = \frac{\partial E_2}{\partial t} = 0, \qquad \frac{\partial B_3}{\partial t} = -\frac{\partial E_2}{\partial x_1}.$$

It is clear that the electric field does not depend on time and the magnetic field changes linearly along the time. Thus the Fourier-transformed fields $\hat{E}_{1,k}(t)$ and $\hat{E}_{2,k}(t)$ stay constant, and the magnetic field $\hat{B}_3$ can be expressed as

$$\hat{B}_{3,k}(t) = \hat{B}_{3,k}(0) - \frac{2\pi i k}{L} t \hat{E}_{2,k}(0), \quad k = -M/2 + 1, \cdots, M/2.$$

As in the previous section, the distribution function f can be computed by translating in two velocity directions. The quantities of the electromagnetic fields at some grid points can be obtained by using the inverse Fourier transform. Details of the procedure for computing $f(x_1, v_1, v_2, t)$ for subsystem $\mathcal{H}_E$ are listed in Algorithm 1.

Subsystem of $\mathcal{H}_{1f}$. The subsystem corresponding to $\mathcal{H}_{1f}$ is

$$\frac{\partial f}{\partial t} + v_1 \frac{\partial f}{\partial x_1} - v_1 B_3 \frac{\partial f}{\partial v_2} = 0, \qquad \frac{\partial E_1}{\partial t} = -\int v_1 f \, dv_1 \, dv_2, \qquad \frac{\partial E_2}{\partial t} = \frac{\partial B_3}{\partial t} = 0.$$

As in (29), we can compute the distribution function by translating $f(x_1, v_1, v_2, 0)$ in the v_2 and x_1-directions. The procedure is listed in Algorithm 2.

By using (29), we can express the electric field E_1 as

$$E_1(x_1,t) = E_1(x_1,0) - \int_0^t \int_{\Omega_v} v_1 \mathcal{S}^{1f}_{x_1}(\tau)\mathcal{S}^{1f}_{v_2}(\tau) f(x_1,v_1,v_2,0)\, dv_1\, dv_2\, dt.$$

The computation of E_1 is as follows. When $k \neq 0$, we have

$$\begin{aligned}
\hat{E}_{1,k}(t) &= \hat{E}_{1,k}(0) - \Delta v_1 \Delta v_2 \sum_{\ell_1}\sum_{\ell_2} \int_0^t \hat{f}^3_{k,\ell_1,\ell_2}(\tau) v_{\ell_1}\, d\tau \\
&= \hat{E}_{1,k}(0) - \Delta v_1 \Delta v_2 \sum_{\ell_1}\sum_{\ell_2} \int_0^t \hat{f}^2_{k,\ell_1,\ell_2} \exp\left(-\frac{2\pi \mathrm{i}}{L} k\tau v_{\ell_1}\right) v_{\ell_1}\, d\tau \qquad (39) \\
&= \hat{E}_{1,k}(0) + \frac{\Delta v_1 \Delta v_2 L}{2\pi \mathrm{i} k} \sum_{\ell_1}\sum_{\ell_2} \hat{f}^2_{k,\ell_1,\ell_2} \left[\exp\left(-\frac{2\pi \mathrm{i}}{L} k t v_{\ell_1}\right) - 1\right],
\end{aligned}$$

where $\hat{f}^2_{k,\ell_1,\ell_2}$ and $\hat{f}^3_{k,\ell_1,\ell_2}$ are defined in steps 8 and 13 in Algorithm 2.
For $k = 0$, we simply have

$$\begin{aligned}
\hat{E}_{1,0}(t) &= \hat{E}_{1,0}(0) - \Delta v_1 \Delta v_2 \sum_{\ell_1}\sum_{\ell_2} \int_0^t \hat{f}^3_{0,\ell_1,\ell_2}(\tau) v_{\ell_1}\, d\tau \\
&= \hat{E}_{1,0}(0) - t\Delta v_1 \Delta v_2 \sum_{\ell_1}\sum_{\ell_2} \hat{f}^2_{0,\ell_1,\ell_2} v_{\ell_1}.
\end{aligned}$$

5. Numerical experiments

The computation of physical problems in plasma are numerically challenging. Even though the initial value of physical problem is perfectly smooth, the multi-scale nature of problem may bring difficulties in simulating small-scale structures. In this section, the numerical discretizations discussed above are applied to simulate several numerical experiments including Landau damping, Weibel instability, and Bernstein wave. The accuracy order in time and comparison with semi-Lagrangian method are also presented.

Landau damping. Landau damping is a physical phenomenon in unmagnetized plasma which was predicted by Landau in 1946 and shown experimentally by Malmberg and Wharton in 1964. The experiment reveals that even without the particle collisions the amplitude of waves can also decrease

Algorithm 2 Procedure for computing $f(\mathbf{x}, \mathbf{v}, t)$ of subsystem $\mathcal{H}_{1f}$

Input: $f_{j,\ell_1,\ell_2}(0), \hat{B}_3(0)$

obtain trigonometric polynomial

$$B_3(x_1) = \sum_{k=-\frac{M}{2}+1}^{\frac{M}{2}-1} \hat{B}_{3,k}(0) \exp\left(\frac{2\pi \mathrm{i} k}{L} x_1\right) + \hat{B}_{\frac{M}{2}}(0) \cos\left(\frac{\pi M}{L} x_1\right)$$

for $j = 1$ to M **do**
  for $\ell_1 = 1$ to N_1 **do**
    compute $\alpha = \int_{x_j}^{x_j + t v_{\ell_1}} B_3(\xi) d\xi$ from $B_3(x_1)$
    obtain $f_{j,\ell_1}(v_2)$ by using PSM with $[f_{j,\ell_1,1}(0), \ldots, f_{j,\ell_1,N_2}(0)]$
    obtain $f_{j,\ell_1}(v_2 + \alpha)$ by translating $f_{j,\ell_1}(v_2)$
    obtain f^1_{j,ℓ_1,ℓ_2} by averaging $f_{j,\ell_1}(v_2 + \alpha)$ over each v_2-cell
  end for
end for
for $\ell_1 = 1$ to N_1 **do**
  for $\ell_2 = 1$ to N_2 **do**
    take fast Fourier transform of f^1_{j,ℓ_1,ℓ_2} and denote result by $\hat{f}^2_{k,\ell_1,\ell_2}$
    obtain $\hat{f}^3_{k,\ell_1,\ell_2}$ by translating $\hat{f}^2_{k,\ell_1,\ell_2}$ in the x_1-direction:
    $\hat{f}^3_{0,\ell_1,\ell_2} = \hat{f}^2_{0,\ell_1,\ell_2}$ and $\hat{f}^3_{k,\ell_1,\ell_2}(t) = \hat{f}^2_{k,\ell_1.\ell_2} \exp(-\frac{2\pi \mathrm{i}}{L} k t v_{\ell_1})$
    compute $f_{j,\ell_1,\ell_2}(t)$ by taking the inverse FFT of $\hat{f}^3_{k,\ell_1,\ell_2}$
  end for
end for

Output: $f_{j,\ell_1,\ell_2}(t)$

rapidly with time. During that process, the energy between electric waves and particles is exchanged.

In the zero-magnetic limit, the $1+\frac{1}{2}$ dimensional Vlasov–Maxwell system reduces to the following Vlasov–Poisson system,

$$\begin{aligned}
&\frac{\partial f}{\partial t}+v_1\frac{\partial f}{\partial x_1}+E_1\frac{\partial f}{\partial v_1}+E_2\frac{\partial f}{\partial v_2}=0,\\
&\frac{\partial E_1}{\partial t}=-\int v_1 f\,dv_1\,dv_2, \quad \frac{\partial E_2}{\partial t}=-\int v_2 f\,dv_1\,dv_2,\\
&\frac{\partial E_1}{\partial x_1}=\int f\,dv_1\,dv_2-1, \quad \frac{\partial E_2}{\partial x_1}=0.
\end{aligned} \tag{40}$$

In the following proposition, we present the dispersion relation for linear Landau damping.

Proposition 5.1. *[23, 36] With a small perturbation of the Fourier mode* $\exp(\mathrm{i}(kx-\omega t))$*, we can derive the dispersion relation for linear Landau damping which is*

$$D(\omega,k)=1+\frac{1}{k^2}\left[1+\sqrt{\frac{\pi}{2}}\frac{\omega}{k}e^{-\frac{\omega^2}{2k^2}}\left(\mathrm{I}-\frac{2}{\sqrt{\pi}}\int_0^{\frac{\omega}{\sqrt{2}k}}e^{t^2}dt\right)\right]=0, \tag{41}$$

where ω *is the frequency and* k *is the wave number.*

Following [9], we consider the Vlasov–Poisson equations (40) on the domain $\Omega=[0,2\pi/k]\times[-5,5]\times[-5,5]$. Periodic boundary conditions are imposed in both the x and v-directions. The initial values are

$$f(x_1,v_1,v_2)=\frac{1}{2\pi}\mathrm{e}^{-\frac{v_1^2+v_2^2}{2}}\left(1+\alpha\cos(kx_1)\right), E_1(x_1)=\frac{\alpha}{k}\sin\left(kx_1\right), E_2(x_1)=0,$$

with wave number $k=0.4$. Here, α measures the size of the perturbation: $\alpha=0.01$ for linear Landau damping and $\alpha=0.5$ for nonlinear Landau damping. We discretize the problem by using $32\times64\times64$ grid points and time step $\Delta t=0.05$. Taking $k=0.4$ in the dispersion relation (41) gives $\omega=\omega_r+\mathrm{i}\omega_i=\pm1.2850-0.0661\mathrm{i}$, where the real part ω_r represents the frequency and the imaginary part ω_i is the decay rate.

In Fig. 1, we plot the time evolution of the electric energy. The top plot shows the exponential decay of the electric energy for linear Landau damping, which is consistent with the analytic one; The bottom plot shows that for

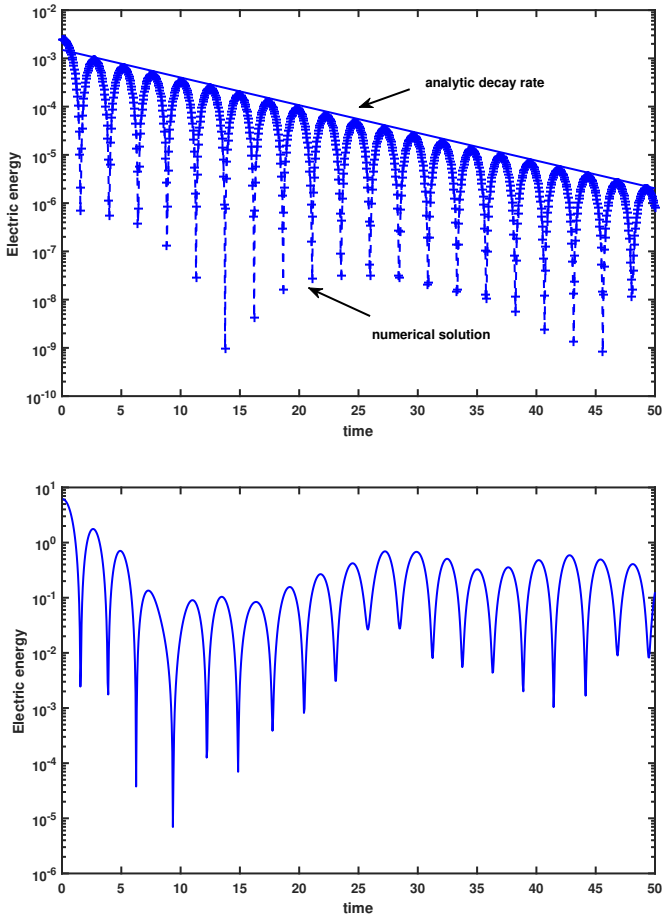

Figure 1: Time evolution of the electric energy for the Landau damping test. The Strang splitting is used. The $32 \times 64 \times 64$ grid points and $\Delta t = 0.05$ time step are used. Top plot: linear Landau damping for $\alpha = 0.01$; Bottom plot: nonlinear Landau damping for $\alpha = 0.5$.

nonlinear Landau damping, the electric energy decays at the beginning for a short time before it starts to oscillate. The time evolution of conserved quantities for nonlinear Landau damping are given in Fig. 2. From these figures, we can see that the conserved quantities are preserved very well: energy error is bounded by about 10^{-2}, charge error is up to 10^{-11}, momentum errors $M_1 = \int v_1 f dx_1 dv_1 dv_2$ is less than 10^{-12} and $M_2 = \int v_2 f dx_1 dv_1 dv_2$ is

preserved to machine precision. We define the discrete Gauss' law,

$$G_j^n = \left(\frac{\partial E_1^n}{\partial x_1}\right)_j - \sum_{\ell_1,\ell_2} f_{j,\ell_1,\ell_2}^n \Delta v_1 \Delta v_2 + 1,$$

where $\left(\frac{\partial E_1^n}{\partial x_1}\right)_j$ is computed by using (inverse) FFT. The l^2 error of discrete Gauss' law is presented in Fig. 3, from which we can see the error is in 10^{-4} level. The contour plots of the distribution function at $v_2 = 0$ are exhibited in Fig. 4. From these plots, it is observed that our method captures finer and finer structures, which verifies the filamentation phenomenon [9].

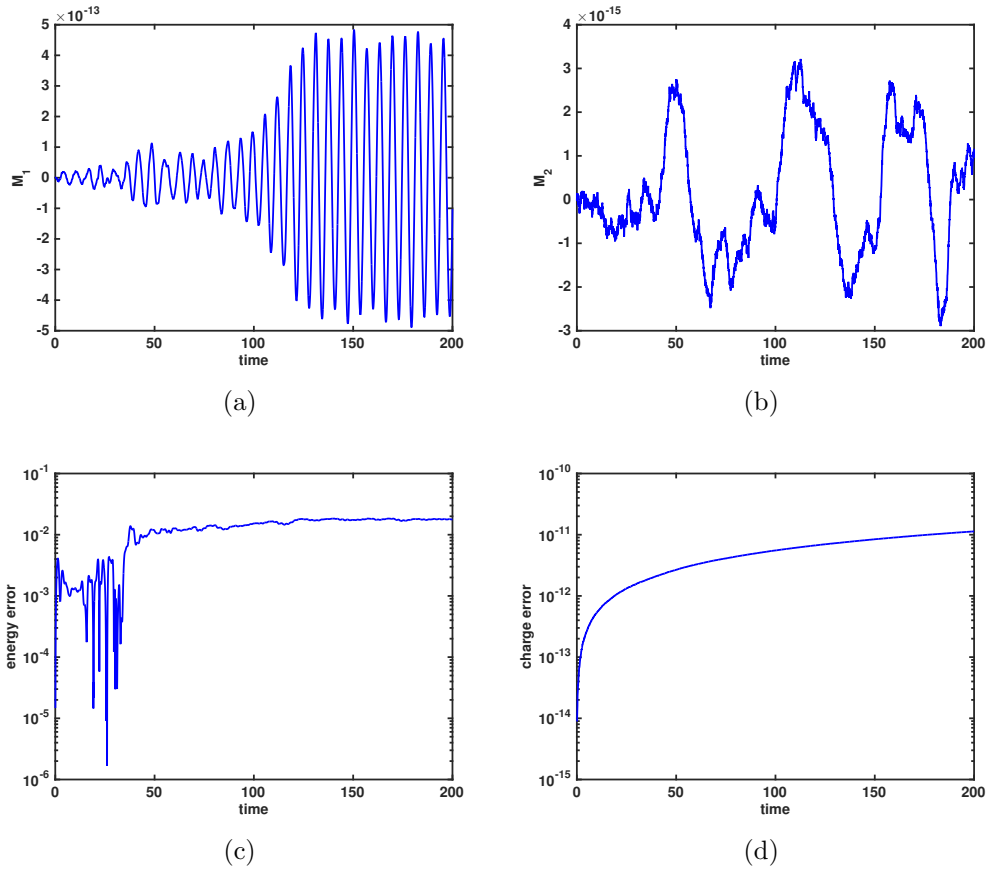

Figure 2: Time evolution of numerical errors by using the Strang splitting with $32\times64\times64$ grid points and a time step of $\Delta t = 0.05$ for nonlinear Landau damping. (a) Momentum M_1; (b) Momentum M_2; (c) Energy; (d) Charge.

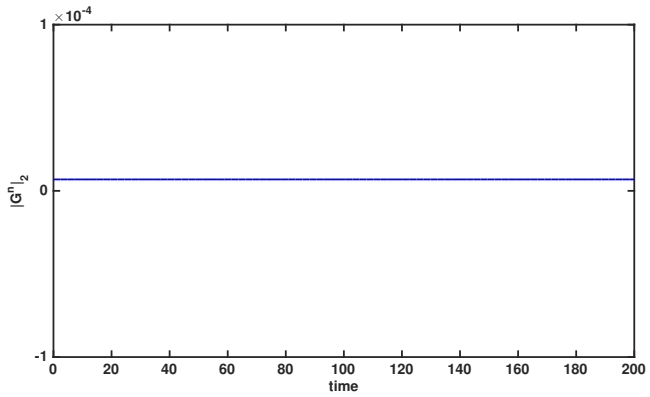

Figure 3: Time evolution of l^2 error of discrete Gauss' law of nonlinear Landau damping.

Run	k_0	β	$v_{0,1}$	$v_{0,2}$	δ	γ_{fluid}	γ_{kin}	Ω_v	grid
1	1	0.002	0.2	0.2	0.5	0.14	0.1350	$[-0.4, 0.4]^2$	$32 \times 64 \times 64$
2	0.2	0.01	0.3	0.3	0.5	0.06	0.0596	$[-1.2, 1.2]^2$	$80 \times 100 \times 100$
3	1	0.01	0.1	0.5	1/6	0.15	0.1207	$[-0.7, 0.7]^2$	$32 \times 64 \times 64$
4	1	0.01	0.3	0.3	0.5	0.21	0.1869	$[-1.0, 1.0]^2$	$32 \times 80 \times 80$

Table 1: Growth rate γ_{kin} corresponding to different parameters of VM equations

.

Weibel instability. The Weibel instability is a very common instability in plasma physics which can be induced by particles with different drift velocities. It has many applications in important magnetic field generation problems. In this example, we study the Weibel instability for two bunches of particles with mean velocities $v_{0,1}$ and $-v_{0,2}$. Initial conditions are taken as follows, in which a small perturbation of size $b = 0.001$ is added to the magnetic field.

$$f(x_1, v_1, v_2) = \frac{1}{\pi\beta} \mathrm{e}^{-\frac{v_1^2}{\beta}} \left(\delta \mathrm{e}^{-\frac{(v_2 - v_{0,1})^2}{\beta}} + (1-\delta) \mathrm{e}^{-\frac{(v_2 + v_{0,2})^2}{\beta}} \right),$$
$$B_3(x_1) = -b \sin(k_0 x_1) \quad \text{and} \quad E_1(x_1) = E_2(x_1) = 0.$$

Here, $\beta^{1/2}$ represents the thermal velocity, δ and $1-\delta$ are the proportion of two bunches of particles. The spatial domain is $\Omega_x = [0, 2\pi/k_0]$ and periodic boundary condition is imposed in both the x- and v- directions.

With step size $\Delta t = 0.1$, we obtain the results which are listed in Table 1. In this table, γ_{fluid} denotes the exponential growth rate obtained by solving

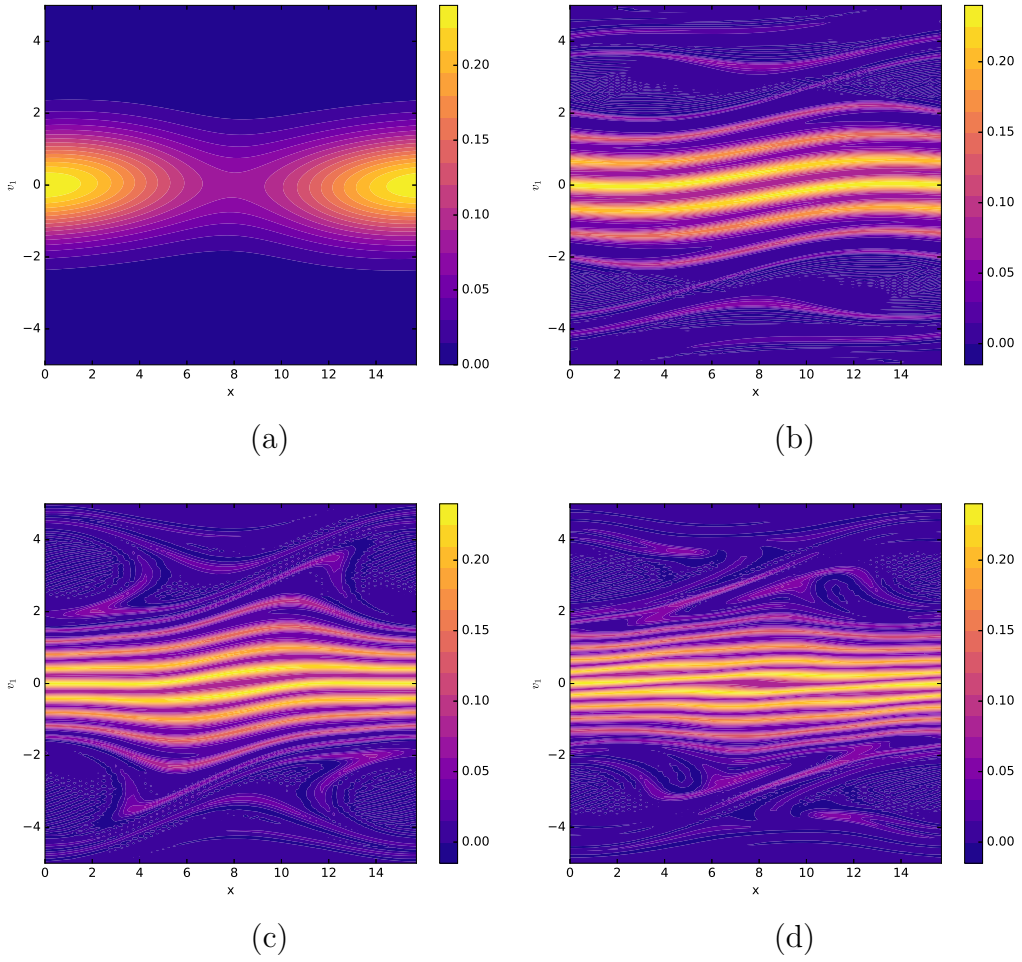

Figure 4: Snapshots of the distribution $f(x, v_1, v_2)$ at $v_2 = -4.98$ for nonlinear Landau damping using the Strang splitting with $64 \times 256 \times 256$ grid points and a time step of $\Delta t = 0.1$. These snapshots are taken at (a) $t = 0$, (b) $t = 20$, (c) $t = 30$ and (d) $t = 40$.

the linear dispersion relation of two-fluid equations [4]; γ_{kin} denotes the exponential growth rate calculated by making a best fit of the numerical energy E_1 in the linear stage of the simulation. Note that in our experiments, β is small, thus γ_{fluid} is a good approximation of γ_{kin}. The data listed in Table 1 shows that our results match the results in [4] very well.

To see the time evolutions of electric energy, magnetic energy, and conserved quantities, we take the first run of Table 1 for example. In this case

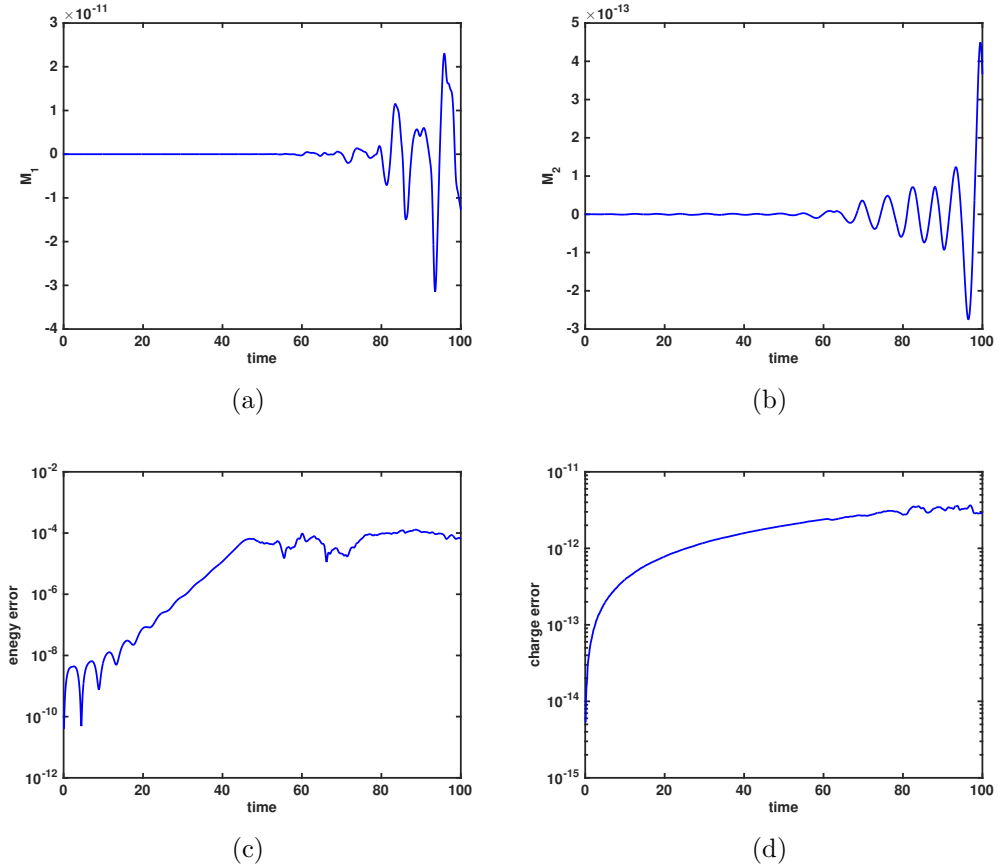

Figure 5: Time evolution of numerical errors by using the Strang splitting with $32\times64\times64$ grid points and a time step of $\Delta t = 0.1$ for Weibel instability. (a) M_1; (b) M_2; (c) Energy; (d) Charge.

we consider two initially symmetric beams with opposite mean velocities: $v_{0,1} = v_{0,2} = 0.2$. The errors of charge, energy, momentums M_1 and M_2 are displayed in Fig. 5. The energy is well conserved with an error of about 10^{-4}, charge error is less than 10^{-11}, M_1, M_2 errors are in 10^{-11} and 10^{-13} levels. Note that in [8] it is mentioned that M_2 is conserved, while M_1 is not. Time evolutions of l^2 error of discrete Gauss law, electric, and magnetic energies are presented in Fig. 5. We can see that the discrete Gauss' law error is less than 10^{-8}. It is investigated that after a rapid transient up to $t \approx 10$, the magnetic energy begins to grow exponentially. About $t = 40$, due to that kinetic effects play a role the instability saturates. The magnetic energy

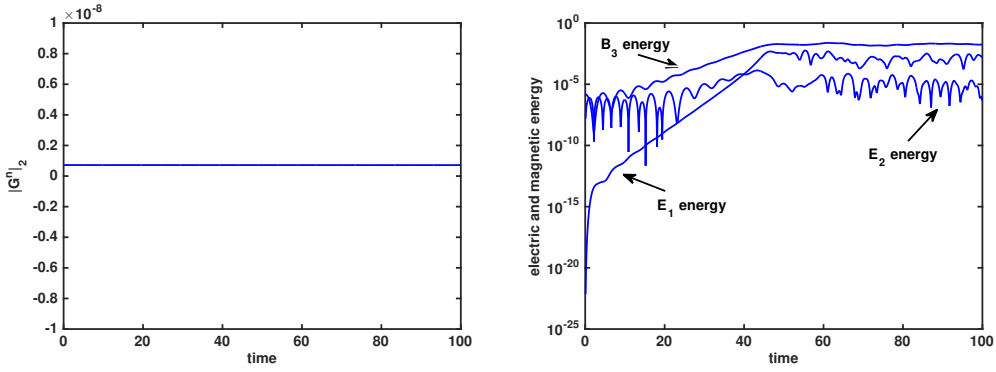

(a) (b)

Figure 6: (a) l^2 error of discrete Gauss' law; (b) electric and magnetic energies for Weibel instability.

becomes nearly constant, and the electric energy reaches its maximum value and then starts to decrease.

With grids $64 \times 64 \times 64$ in phase space, we compute the sum of l^1 errors of E_1, E_2, and B_3 at time $T = 1$ with respect to different step sizes, and the accuracy orders in time are presented in Table 2. The reference solution here is obtained by using the same grids in space with sufficiently small steps. From Table 2, it can be seen that the numerical discretizations of order 1, 2 and 4 can be achieved by using Lie splitting, Strang splitting, and triple jump splitting respectively.

Dispersion of electron Bernstein wave. The study on physics of the propagation of electron Bernstein wave has a long history, and has been applied in a wide range of fields including magnetically confined plasma, astrophysics, and so on. In plasma physics, waves are usually induced by the interaction between particles and electromagnetic fields. The electron Bernstein wave is a high-frequency electrostatic kinetic mode, especially in hot magnetized plasma. In order to analyze the dispersion relation of Bernstein wave [43], one needs to linearize the system around an equilibrium state with a zero electric field and a uniform externally applied magnetic field. For the linearized equation, we use the Fourier–Laplace transform to give the dispersion relation which characterizes the Bernstein wave. For our reduced system (30)–(33), the dispersion relation relating to the perpendicular wave

Method	Time step	l^1 error	Order
Lie splitting	0.2	6.007615595650e-3	
	0.1	3.073091845594e-3	0.96710
	0.05	1.555971830528e-3	0.98187
	0.025	7.831142475281976e-4	0.99052
	0.0125	3.928739010065202e-4	0.99516
Strang splitting	0.2	2.759504011978908e-4	
	0.1	6.881116555789667e-5	2.00369
	0.05	1.719180558077524e-5	2.00092
	0.025	4.297269224821313e-5	2.00023
	0.0125	1.074277896159182e-5	2.00005
Triple jump splitting	0.05	6.817763274516141e-9	
	0.025	4.286143175725143e-10	3.99155
	0.0125	2.70765293391800e-11	3.98457

Table 2: Accuracy order in time by Lie splitting, Strang splitting, and triple jump splitting method.

number k and the plasma wave frequency ω of Bernstein waves is [39]:

$$\begin{vmatrix} 1-\mathrm{M}\frac{\mathrm{e}^{-\lambda}}{\lambda\omega}\sum\limits_{n=-\infty}^{\infty}A_n & \mathrm{iM}\frac{\mathrm{e}^{-\lambda}}{\omega}\sum\limits_{n=-\infty}^{\infty}B_n \\ -\mathrm{iM}\frac{\mathrm{e}^{-\lambda}}{\omega}\sum\limits_{n=-\infty}^{\infty}B_n & 1-\frac{\lambda}{\omega^2}\frac{c^2}{\mathrm{M}^2v_{\mathrm{T}}^2}-\mathrm{M}\frac{\mathrm{e}^{-\lambda}}{\lambda\omega}\sum\limits_{n=-\infty}^{\infty}C_n \end{vmatrix} = 0,$$

where $A_n = n^2 I_n(\lambda)/(\omega\mathrm{M}-n)$, $B_n = (n(I_n'(\lambda) - I_n(\lambda)))/(\omega\mathrm{M}-n)$, $C_n = (n^2 I_n(\lambda) + 2\lambda^2 I_n(\lambda) - 2\lambda^2 I_n'(\lambda))/(\omega\mathrm{M}-n)$. Here, I_n is the modified Bessel function of first kind, $\lambda = (5.83696\cdot 10^{-3})k^2$, v_{T} denotes the thermal velocity and $M = 1.2736$. We truncate the above equality at sufficiently large n.

Consider the $1+1/2$ dimensional Vlasov–Maxwell system on $\Omega = [0,12]\times[-0.4,0.4]\times[-0.4,0.4]$. The initial value is chosen as

$$f(x_1,v_1,v_2) = \frac{1}{T_r^2\pi}\mathrm{e}^{-\frac{v_1^2+v_2^2}{v_{\mathrm{T}}^2}}\left(1+a\sum_{n=1}^{s}n\cos(\frac{\pi}{6}nx)\right),$$

$$E_1 = \frac{6a}{\pi}\sum_{n=1}^{s}\sin\left(\frac{\pi}{6}nx\right), \quad E_2 = 0, \quad \text{and} \quad B_3 = 0.785,$$

where s represents the number of modes which is taken as $s = 60$ in order to obtain the accurate Bernstein wave, $a = 10^{-7}$ denotes the size of the perturbation, and thermal velocity $v_{\mathrm{T}} = \sqrt{0.0072}$. Periodic boundary conditions are imposed both in the x- and v-directions. The numerical computation is

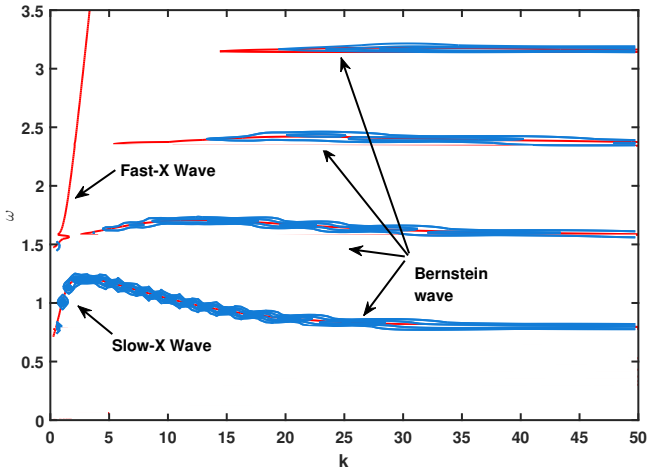

Figure 7: The dispersion relation of the Bernstein wave. Red lines represent the analytic results and blue curves represent the numerical results.

done over the time interval $[0, 30\pi]$ with step size $\Delta t = 0.02$. We use the Lie splitting method in time and take the spatial grids as $256 \times 64 \times 64$. We demonstrate the numerical Bernstein wave in Fig. 7. From the plot, it is observed that our numerical dispersion relation of Bernstein wave is perfectly consistent with the analytical one.

The errors of moments M_1 and M_2, the charge, the energy are listed in Fig. 8, in which we can see that these quantities are preserved very well on the discrete level. We also plot the time evolution of l^2 error of discrete Gauss law in Fig. 5, which is less than 10^{-8} and conserved for long time.

Comparison of cost with semi-Lagrangian method. As follows, the computational costs between semi-Lagrangian method and Hamiltonian splitting method (Lie splitting) are compared. Here 1D and high dimensional cubic spline methods [37] are used for Hamiltonian splitting method and semi-Lagrangian method respectively. It is pointed out in paper [19] that the semi-Lagrangian method is extremely expensive for solving the high dimensional problem because of the multi-dimensional interpolation. Compared with this, the Hamiltonian splitting method only needs one-dimensional interpolation. Specifically, for a problem of d-dimension a typical cubic spline evaluation involves a stencil of 4^d points which grows very fast when d be-

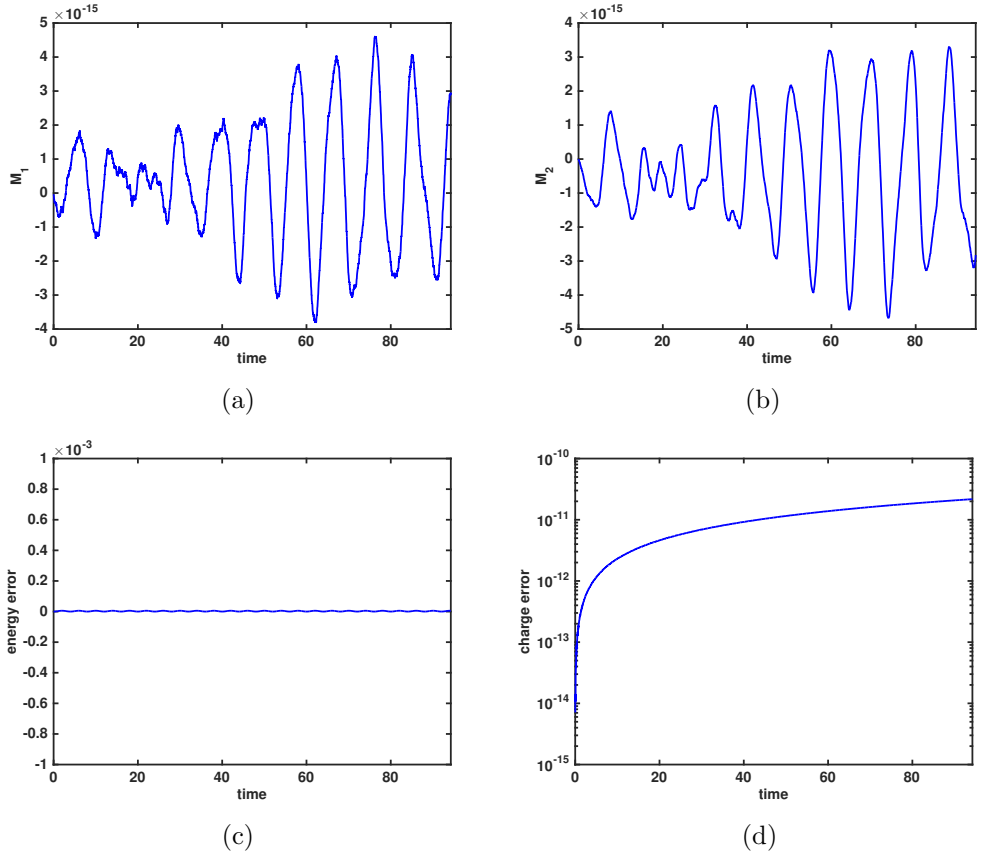

Figure 8: Errors of conserved quantities by using the Lie splitting with $256 \times 64 \times 64$ grid points and a time step of $\Delta t = 0.02$ for Bernstein wave. (a) M_1; (b) M_2; (c) Energy; (d) Charge.

comes large. By applying the fast solver to the linear system of cubic spline interpolation [36], the computation cost of interpolation in the Hamiltonian splitting method (e.g. Lie splitting) is $\mathcal{O}(N^d)$, while the computation cost for the interpolation part in the semi-Lagrangian method is $4^d\mathcal{O}(N^d)$. Here, we compare the Hamiltonian splitting method and semi-Lagrangian method for 2D problem and 3D problem. As the computation cost mainly comes from the Vlasov equation, here we assume that the electromagnetic field is given. In this case, the 2D problem is reduced to $\frac{\partial f}{\partial t} + v\frac{\partial f}{\partial x} + E(x)\frac{\partial f}{\partial v} = 0$, and the 3D problem is written in (30). By using the same number of grids and periodic boundary conditions in $\mathbf{x}$ and $\mathbf{v}$, the computation costs over 100 steps are presented in Fig.10. From Fig.10 we can see that the Hamiltonian

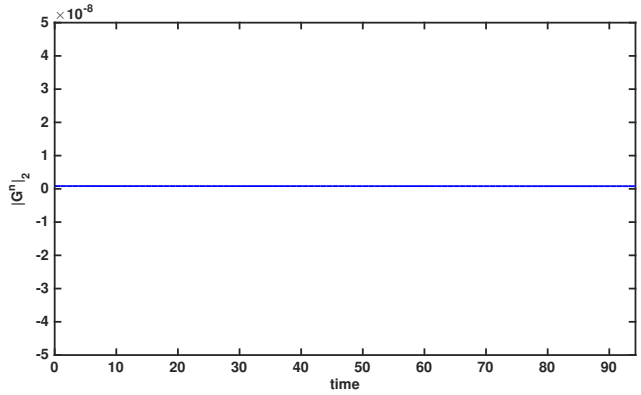

Figure 9: Time evolution of l^2 error of discrete Gauss' law of Bernstein wave.

splitting method is more efficient, and its efficiency is more obvious for higher dimensional problems, although there are more subsystems to compute for Hamiltonian splitting method. Recently the idea that computing the solution of distribution function by several 1D translations has been used in six dimensional Vlasov–Poisson system [24].

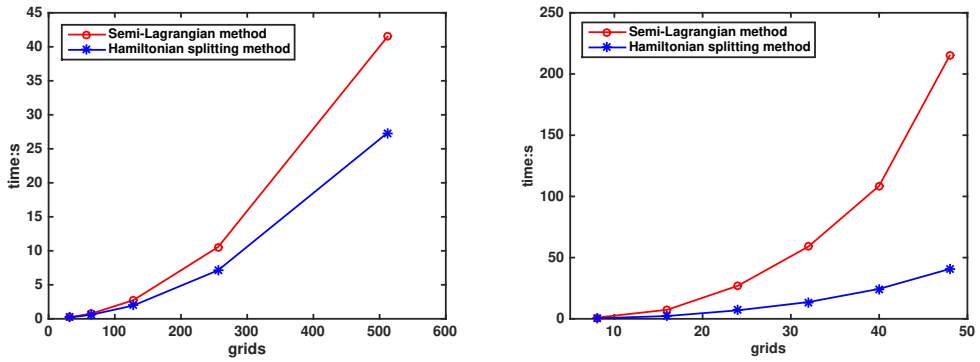

(a) (b)

Figure 10: Comparison of costs between semi-Lagrangian method and Hamiltonian splitting method by running 100 steps. (a) 2D problem; (b) 3D problem.

6. Conclusion

In this paper, we proposed a Hamiltonian splitting method based on the Morrison–Marsden–Weinstein Poisson bracket. With this bracket, we describe the Vlasov–Maxwell system in a Poisson bracket formulation. Then the Hamiltonian of the Vlasov–Maxwell system is split into five parts, yielding five Hamiltonian subsystems. By composing the solutions of the five subsystems which can be written out explicitly, we get an approximate solution of the original system which preserves the Poisson structure and satisfies Gauss's law. Moreover the solution of distribution function in each subsystem can be expressed by several one dimensional translations. This makes the computation of numerical solutions more efficient. In phase space, we use the Fourier spectral method and finite volume method. Numerical simulations show that our method gives accurate results in various standard test settings.

There are several future perspectives for this research. In numerical simulation, it should be quite natural to implement parallel computation, as only 1D translations are needed for solving the Vlasov equation. Furthermore, we can obtain more efficient high-order numerical discretization in time by optimizing the composition coefficients as in [5].

Acknowledgements

This research was supported by the National Natural Science Foundation of China (11771436, 11261140328, 11305171), by the CAS Program for Interdisciplinary Collaboration Team, the Foundation for Innovative Research Groups of the NNSFC (11321061), the ITER-China Program (2014GB124005, 2015GB111003), JSPS-NRF-NSFC A3 Foresight Program in the field of Plasma Physics (NSFC-11261140328), and Royal Society (London) (IE141408).

[1] C. K. Birdsall and A. B. Langdon. *Plasma Physics Via Computer Simulation*. Institute of Physics Publishing, Philadelphia, PA, 1991.

[2] K. J. Bowers, B. J. Albright, L. Yin, B. Bergen, and T. J. T. Kwan. Ultrahigh performance three-dimensional electromagnetic relativistic kinetic plasma simulation. *Physics of Plasmas*, 15(5):199–434, 2008.

[3] M. Caliari, A. Ostermann, and C. Piazzola. A splitting approach for the magnetic Schrödinger equation. *Journal of Computational and Applied Mathematics*, 316, 2016.

[4] F. Califano, F. Pegoraro, S. V. Bulanov, and A. Mangeney. Kinetic saturation of the Weibel instability in a collisionless plasma. *Physical Review E*, 57(6):7048–7059, 1998.

[5] F. Casas, N. Crouseilles, E. Faou, and M. Mehrenberger. High-order Hamiltonian splitting for the Vlasov-Poisson equations. *Numerische Mathematik*, 135(3):769–801, 2017.

[6] Y. Cheng, A. J. Christlieb, and X. Zhong. Energy-conserving discontinuous Galerkin methods for the Vlasov-Ampère system. *Journal of Computational Physics*, 256:630–655, 2014.

[7] Y. Cheng, A. J. Christlieb, and X. Zhong. Energy-conserving discontinuous Galerkin methods for the Vlasov–Maxwell system. *Journal of Computational Physics*, 279:145–173, 2014.

[8] Y. Cheng, I. M. Gamba, F. Li, and P. J. Morrison. Discontinuous Galerkin Methods for the Vlasov–Maxwell Equations. *SIAM Journal on Numerical Analysis*, 52(2):1017–1049, 2014.

[9] N. Crouseilles, L. Einkemmer, and E. Faou. Hamiltonian splitting for the Vlasov-Maxwell equations. *Journal of Computational Physics*, 283:224–240, 2015.

[10] N. Crouseilles, M. Mehrenberger, and E. Sonnendrucker. Conservative semi-Lagrangian schemes for Vlasov equations. *Journal of Computational Physics*, 229(6):1927–1953, 2010.

[11] J. M. Dawson. Particle simulation of plasmas. *Reviews of Modern Physics*, 55(2):403–447, 1983.

[12] R. J. Diperna and P. Lions. Global weak solutions of Vlasov-Maxwell systems. *Communications on Pure and Applied Mathematics*, 42(6):729–757, 1989.

[13] L. Einkemmer and A. Ostermann. Convergence analysis of a discontinuous Galerkin/Strang splitting approximation for the Vlasov–Poisson equations. *SIAM Journal on Numerical Analysis*, 52(2):757–778, 2014.

[14] E. Evstatiev and B. Shadwick. Variational formulation of particle algorithms for kinetic plasma simulations. *Journal of Computational Physics*, 245(6):376–398, 2013.

[15] E. Faou. Geometric Numerical Integration and Schrödinger Equations. *Springer Indam*, 25(1):805–882, 2012.

[16] K. Feng and M. Qin. *Symplectic Geometric Algorithms for Hamiltonian Systems*. Springer Berlin Heidelberg, 2010.

[17] F. Filbet. Convergence of a Finite Volume Scheme for the Vlasov-Poisson System. *SIAM Journal on Numerical Analysis*, 39(4):1146–1169, 2002.

[18] F. Filbet, E. Sonnendrücker, and P. Bertrand. Conservative numerical schemes for the Vlasov equation. *Journal of Computational Physics*, 172(1):166–187, 2001.

[19] V. Grandgirard, J. Abiteboul, J. Bigot, T. Cartier-Michaud, N. Crouseilles, G. Dif-Pradalier, C. Ehrlacher, D. Esteve, X. Garbet, P. Ghendrih, et al. A 5D gyrokinetic full-f global semi-lagrangian code for flux-driven ion turbulence simulations. *Computer Physics Communications*, 207:35–68, 2016.

[20] E. Hairer, C. Lubich, and G. Wanner. *Geometric numerical integration: structure-preserving algorithms for ordinary differential equations*, volume 31. Springer Science & Business Media, 2006.

[21] Y. He, Y. Sun, J. Liu, and H. Qin. Volume-preserving algorithms for charged particle dynamics. *Journal of Computational Physics*, 281:135–147, 2015.

[22] Y. He, Y. Sun, R. Zhang, Y. Wang, J. Liu, and H. Qin. High order volume-preserving algorithms for relativistic charged particles in general electromagnetic fields. *Physics of Plasmas*, 23(9):092109, 2016.

[23] R. E. Heath, I. M. Gamba, P. J. Morrison, and C. Michler. A discontinuous Galerkin method for the Vlasov-Poisson system. *Journal of Computational Physics*, 231(4):1140–1174, 2012.

[24] K. Kormann, K. Reuter, and M. Rampp. A massively parallel semi-Lagrangian solver for the six-dimensional Vlasov–Poisson equation. *The International Journal of High Performance Computing Applications*, page 1094342019834644, 2019.

[25] M. Kraus, K. Kormann, P. J. Morrison, and E. Sonnendrücker. GEMPIC: geometric electromagnetic particle-in-cell methods. *Journal of Plasma Physics*, 83(04), 2017.

[26] G. Manzini, G. L. Delzanno, J. Vencels, and S. Markidis. A Legendre Fourier spectral method with exact conservation laws for the Vlasov-Poisson system. *Journal of Computational Physics*, 317(C):82–107, 2016.

[27] J. E. Marsden and A. Weinstein. The Hamiltonian structure of the Maxwell-Vlasov equations. *International symposium on physical design*, 4(3):394–406, 1982.

[28] R. I. Mclachlan and G. R. W. Quispel. Splitting methods. *Acta Numerica*, 11(11):341–434, 2002.

[29] P. J. Morrison. The Maxwell-Vlasov equations as a continuous Hamiltonian system. *Physics Letters A*, 80:383–386, 1980.

[30] P. J. Morrison. A general theory for gauge-free lifting. *Physics of Plasmas*, 20(1):012104, 2013.

[31] H. Qin, Y. He, R. Zhang, J. Liu, J. Xiao, and Y. Wang. Comment on Hamiltonian splitting for the Vlasov–Maxwell equations. *Journal of Computational Physics*, 297:721–723, 2015.

[32] H. Qin, J. Liu, J. Xiao, R. Zhang, Y. He, Y. Wang, Y. Sun, J. W. Burby, L. Ellison, and Y. Zhou. Canonical symplectic particle-in-cell method for long-term large-scale simulations of the Vlasov-Maxwell equations. *Nuclear Fusion*, 56(1):014001, 2016.

[33] R. Quispel and R. I. Mclachlan. Geometric Numerical Integration of Differential Equations. *Journal of Physics A*, 39(19), 2006.

[34] R. D. Ruth. A Canonical Integration Technique. *IEEE Transactions on Nuclear Science*, 30(4):2669–2671, 1983.

[35] N. J. Sircombe and T. D. Arber. VALIS: A split-conservative scheme for the relativistic 2D Vlasov-Maxwell system. *Journal of Computational Physics*, 228(13):4773–4788, 2009.

[36] E. Sonnendrücker. *Numerical Methods for the Vlasov-Maxwell Equations*. Springer, 2017.

[37] E. Sonnendrucker, J. Roche, P. Bertrand, and A. Ghizzo. The Semi-Lagrangian Method for the Numerical Resolution of the Vlasov Equation. *Journal of Computational Physics*, 149(2):201–220, 1999.

[38] J. Squire, H. Qin, and W. M. Tang. Geometric integration of the Vlasov-Maxwell system with a variational particle-in-cell scheme. *Physics of Plasmas*, 19(8):084501, 2012.

[39] T. H. Stix. *Waves in Plasmas*. Springer, New York, 1992.

[40] M. Suzuki. General theory of higher-order decomposition of exponential operators and symplectic integrators. *Physics Letters A*, 165:387–395, 1992.

[41] A. Weinstein and P. J. Morrison. Comments on: The Maxwell-Vlasov equations as a continuous hamiltonian system. *Physics Letters A*, 86(4):235–236, 1981.

[42] S. Wollman. Local existence and uniqueness theory of the Vlasov-Maxwell system. *Journal of Mathematical Analysis and Applications*, 127(1):103–121, 1987.

[43] J. Xiao, J. Liu, H. Qin, and Z. Yu. A variational multi-symplectic particle-in-cell algorithm with smoothing functions for the Vlasov-Maxwell system. *Physics of Plasmas*, 20(10):2669–37, 2013.

[44] J. Xiao, H. Qin, J. Liu, Y. He, R. Zhang, and Y. Sun. Explicit high-order non-canonical symplectic particle-in-cell algorithms for Vlasov-Maxwell systems. *Physics of Plasmas*, 22(11):112504, 2015.

[45] H. Yoshida. Construction of higher order symplectic integrators. *Physics Letters A*, 150:262–268, 1990.

[46] M. Zerroukat, N. Wood, and A. Staniforth. The Parabolic Spline Method (PSM) for conservative transport problems. *International Journal for Numerical Methods in Fluids*, 51(11):1297–1318, 2006.